Tectonophysics 863 (2023) 230010

Contents lists available at ScienceDirect

Tectonophysics

journal homepage: www.elsevier.com/locate/tecto

A critical reappraisal of paleomagnetic evidence for Philippine Sea Plate rotation

Suzanna H.A. van de Lagemaat [a,*], Daniel Pastor-Galán [b,c], Bas B.G. Zanderink [a], Maria J.Z. Villareal [d], John W. Jenson [d], Mark J. Dekkers [a], Douwe J.J. van Hinsbergen [a]

[a] Department of Earth Sciences, Utrecht University, the Netherlands
[b] Department of Geodynamics, Universidad de Granada, Spain
[c] Frontier Research Institute for Interdisciplinary Sciences, Tohoku University, Japan
[d] Water Environmental Research Institute of the Western Pacific, University of Guam, USA

ARTICLE INFO

Keywords:
Paleomagnetism
Guam
Philippine Sea Plate
Philippines
Philippine Mobile Belt
Izu-Bonin Mariana forearc

ABSTRACT

The kinematic history of the Philippine Sea Plate (PSP) is crucial for interpreting its geological record related to subduction initiation processes and the paleogeography of the junction between the Paleo-Pacific and Tethyan oceanic realms. However, reconstructing PSP's kinematic history is difficult because the plate has been surrounded by subduction zones for most of its history. In absence of marine magnetic anomalies to constrain PSP's motion relative to its neighboring plates, paleomagnetic data may be used as quantitative constraints on its motion. Previous paleomagnetic studies interpreted easterly deflected declinations to infer clockwise rotations of up to 90° since the Eocene. However, rotations inferred from these datasets may also reflect local block rotations related to plate margin deformation. We here re-evaluate to what extent paleomagnetic data from the PSP unequivocally demonstrate plate motion rather than local rotation. To this end, we provide new data from Guam, in the Mariana forearc, and reassess published paleomagnetic data. Our new data from Guam come from two localities in the Eocene, two in the Oligocene, and two in the Miocene. Our compilation assesses data quality against recently defined criteria. Our new results demonstrate that in Guam, declination differences of up to 35° exist in rocks of Eocene age, indicating local rotations. Our compilation identifies both clockwise and counterclockwise rotations from the plate margins, with little confidence which of these would reflect plate-wide rotation. We compiled paleolatitude data from igneous rocks, which we correct for microplate rotation constrained by intra-PSP marine magnetic anomalies and show a northward drift of the PSP of ~15° since the Eocene, but without a paleomagnetic necessity for major vertical axis rotation. Hence, with the currently available data, rotations of the PSP may be permitted, but are not required. Plate motion is currently better reconstructed from geological constraints contained in circum-PSP orogenic belts.

1. Introduction

For most of its tectonic history since the Eocene, the Philippine Sea Plate (PSP) and associated microplates have been surrounded by subduction zones (e.g., Hall, 2002; Gaina and Müller, 2007; Wu et al., 2016). Consequently, the reconstruction of the PSP relative to the surrounding major plates of the Pacific, Australia, and Eurasia cannot be determined from marine magnetic anomalies, and reconstruction of its past tectonic motions is challenging. In such cases, paleomagnetic data may provide quantitative constraints on paleolatitude evolution and vertical axis rotation of the plate (e.g., Fuller et al., 1989; Haston and Fuller, 1991; Hall et al., 1995a, 1995b), which may then be incorporated in reconstructions based on geological (e.g., Hall, 2002) or seismic tomographic data (Wu et al., 2016).

The paleomagnetic data from the PSP come from rocks exposed on the plate margins (Fig. 1), i.e., on the Philippines and Halmahera in the west and the islands in the arc and forearc adjacent to the Marianas and Izu-Bonin trenches in the east, as well as from boreholes in the plate interior. Even though the database is extensive (e.g., Louden, 1977; Kinoshita, 1980; Keating and Herrero, 1980; Keating, 1980; Bleil, 1982; Fuller et al., 1989; Haston and Fuller, 1991; Haston et al., 1992; Koyama et al., 1992; Hall et al., 1995a, 1995b; Queaño et al., 2007, 2009;

* Corresponding author.
E-mail address: s.h.a.vandelagemaat@uu.nl (S.H.A. van de Lagemaat).

https://doi.org/10.1016/j.tecto.2023.230010
Received 30 May 2023; Received in revised form 8 August 2023; Accepted 16 August 2023
Available online 20 August 2023

Yamazaki et al., 2010, 2021; Balmater et al., 2015; Richter and Ali, 2015; Liu et al., 2021; Sager and Carvallo, 2022), these sampling locations come with challenges in providing firm constraints on plate motion evolution. The western plate margin is strongly deformed by distributed strike-slip faults and thrusts which makes it difficult to assess whether vertical axis rotations are local or plate-wide (e.g., Queaño et al., 2007). The eastern plate margin is also strongly deformed, e.g., by extensional processes opening forearc and back-arc basins (e.g., Yamazaki et al., 2003; Sdrolias et al., 2004). The drill cores in the plate's interior yielded large paleomagnetic datasets (e.g., Louden, 1977; Kinoshita, 1980; Keating and Herrero, 1980; Keating, 1980; Bleil, 1982; Yamazaki et al., 2010, 2021; Richter and Ali, 2015; Sager and Carvallo, 2022), but these are not azimuthally oriented and can only be used to constrain paleolatitude. As a result, paleomagnetic declinations from the PSP vary widely and it is difficult to establish whether these may be interpreted as representative for rotation of the PSP in its entirety, and which represent local block rotations of the deformed plate margins. Despite the ambiguity in paleomagnetic data interpretation, most models include major clockwise rotation of up to 90° of the PSP, following paleomagnetic constraints (e.g., Haston and Fuller, 1991; Hall et al., 1995a; Deschamps and Lallemand, 2002; Sdrolias et al., 2004; Seton et al., 2012; Wu et al., 2016; Liu et al., 2023), sometimes despite questioning the reliability of paleomagnetic data (Wu et al., 2016). Others chose to not use paleomagnetic data as input for their reinstruction (e.g., Xu et al., 2014), or only to a limited extent (Zahirovic et al., 2014), and therefore those reconstructions include a much smaller rotation or no vertical-axis rotation at all.

While declination data of the PSP may be considered as ambiguous, paleomagnetic studies to obtain inclination data are still useful, as they provide insight into the paleolatitude evolution of the PSP. Published paleomagnetic data are often indicating Eocene paleolatitudes that are about 20° lower than today (e.g., Haston and Fuller, 1991; Hall et al., 1995b; Queaño et al., 2007; Yamazaki et al., 2010), although paleolatitudes obtained from sediments are subject to inclination shallowing. Taking the relative motions of the present and former microplates that together comprise the PSP into account that are reconstructed from marine magnetic anomalies (Hilde and Chao-Shing, 1984; Deschamps and Lallemand, 2002; Yamazaki et al., 2003; Sdrolias et al., 2004), these paleolatitudes provide valuable information on PSP motions.

In this paper, we compile the current state-of-the art of the paleomagnetic database of the PSP and surrounding former and present microplates, and re-evaluate the paleomagnetic evidence for major vertical-axis plate rotation. We report newly collected paleomagnetic data from the island of Guam, located in the forearc of the southernmost portion of the Izu-Bonin Mariana (IBM) subduction zone, whose crust formed shortly after initiation of the present subduction zone in the Eocene (Ishizuka et al., 2011a, 2018; Reagan et al., 2010, 2013, 2019; Hickey-Vargas et al., 2018). We collected samples from Eocene, Oligocene, and Miocene volcanic and sedimentary rocks from Guam. We collected samples from two localities of each epoch to evaluate whether

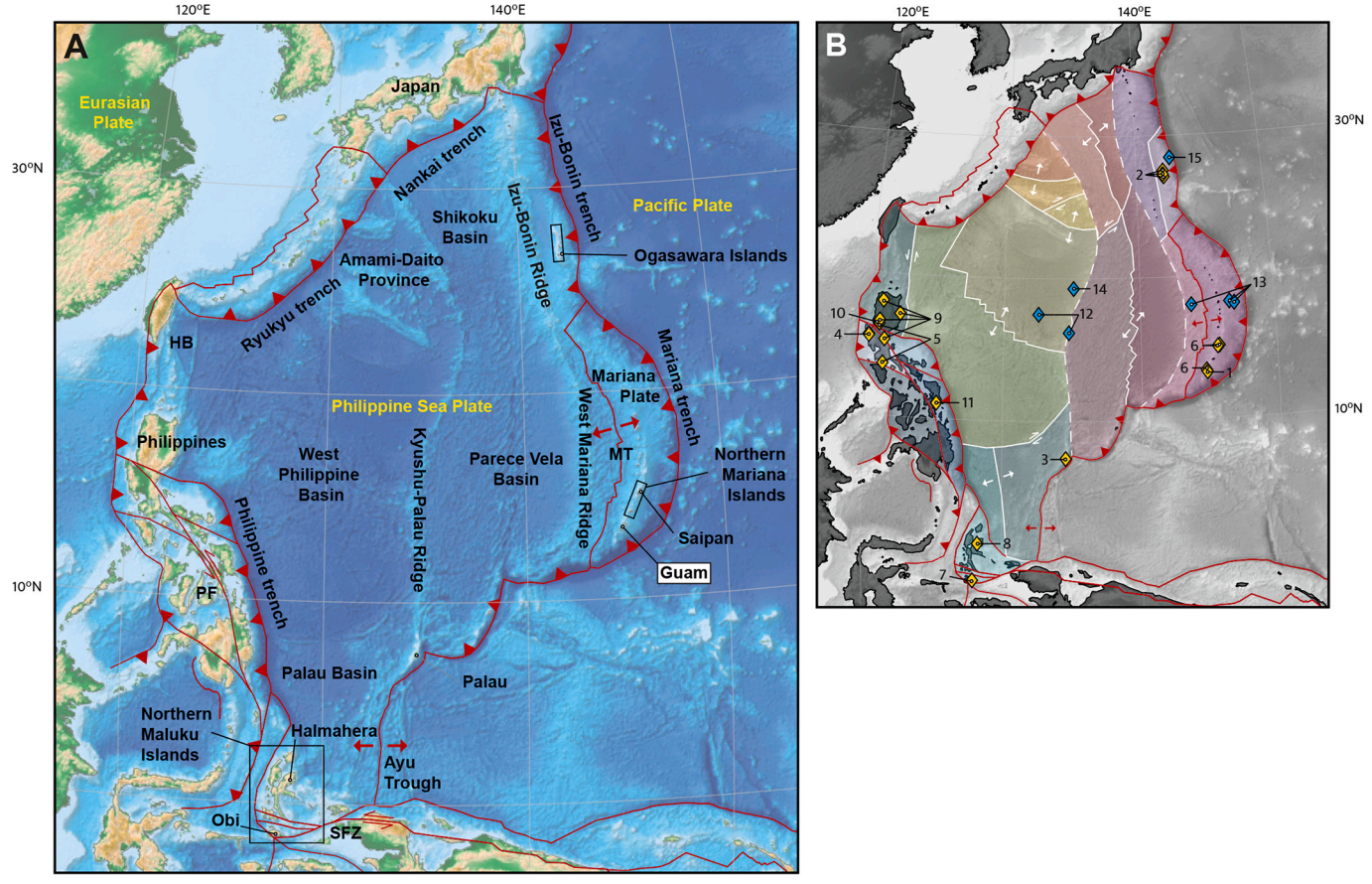

Fig. 1. A) Geographic map of the Philippine Sea Plate region; B) Current and former microplates of the PSP. Current plate boundaries (based on Bird, 2003) in red, former plate boundaries in white (based on marine magnetic anomaly and radiometric age data; see Section 2 for references). Yellow (blue) diamonds on panel B mark sampling locations of previously published paleomagnetic data obtained from igneous rocks in field (borehole) localities, numbered per reference (1) This study; 2) Kodama et al. (1983); 3) Haston et al. (1988); 4) Fuller et al. (1989); 5) Fuller et al. (1991); 6) Haston and Fuller (1991); 7) Ali and Hall (1995); 8) Hall et al., (1995b); 9) Queaño et al. (2007); 10) Queaño et al. (2009); 11) Balmater et al. (2015); 12) Keating and Herrero (1980); 13) Bleil (1982); 14) Richter and Ali (2015); 15) Sager and Carvallo (2022)). Base map is ETOPO, 2022 15 Arc-Second Global Relief Model (NOAA National Centers for Environmental Information, 2022). HB: Huatung Basin; MT: Mariana Trough; PF: Philippine Fault; SFZ: Sorong Fault Zone. (For interpretation of the references to colour in this figure legend, the reader is referred to the web version of this article.)

declinations are coherent on the scale of the island, or whether variations in declination exist in rocks of similar age. We add these data to our compilation of previously published paleomagnetic data from the PSP. We evaluate the reliability of the available paleolatitude constraints using recently defined quality criteria (Meert et al., 2020; Vaes et al., 2021; Gerritsen et al., 2022). We will use these to critically re-evaluate the paleomagnetic constraints on vertical-axis rotation and paleolatitudinal evolution of the PSP.

2. Geological setting

The PSP is in the West Pacific realm and is separated from the Pacific Plate by the Izu-Bonin Mariana subduction zone, where the Pacific Plate is subducting westwards below the PSP (Fig. 1). The PSP contains small remains of Jurassic and Cretaceous ocean floor and arc sequences (e.g., Dimalanta et al., 2020; Yumul Jr et al., 2020; Ishizuka et al., 2022, and references therein), as well as several inactive spreading ridges where the plate's lithosphere grew at different times throughout much of the Cenozoic (Hilde and Chao-Shing, 1984; Deschamps and Lallemand, 2002; Sdrolias et al., 2004). At present, one microplate (the Mariana microplate carrying the Mariana arc, including Guam) is diverging from the PSP, accommodated by oceanic spreading in the Mariana Trough (Fig. 1). This separated the active arc from the now inactive West Mariana Ridge, a remnant volcanic arc that was active until the Miocene (e.g., Yamazaki et al., 2003). To the north, the Mariana Trough spreading center disappears and no oceanic spreading is currently active in the Izu-Bonin ridge region (Fig. 1). The Izu-Bonin Ridge and West Mariana Ridge remnant arcs form the eastern margin of the Shikoku-Parece Vela Basin that hosts former oceanic spreading centers that were simultaneously active in the Oligocene-Miocene (c. 30–15 Ma; Sdrolias et al., 2004; Ishizuka et al., 2010), although different kinematic solutions have been proposed for the formation of each basin (Sdrolias et al., 2004). The western boundary of the Shikoku-Parece Vela Basin is the Kyushu-Palau Ridge, another remnant volcanic arc with magmatic rocks that formed from c. 48 to 25 Ma (Ishizuka et al., 2011b). To the west of the Kyushu-Palau Ridge is the West Philippine Basin (Fig. 1). This basin hosts a fossil spreading center that formed through N-S spreading (in present-day coordinates), between ~54 and 34 Ma (Hilde and Chao-Shing, 1984; Deschamps and Lallemand, 2002). In the north, in the Amamii-Daito Province, the PSP hosts a series of Cretaceous

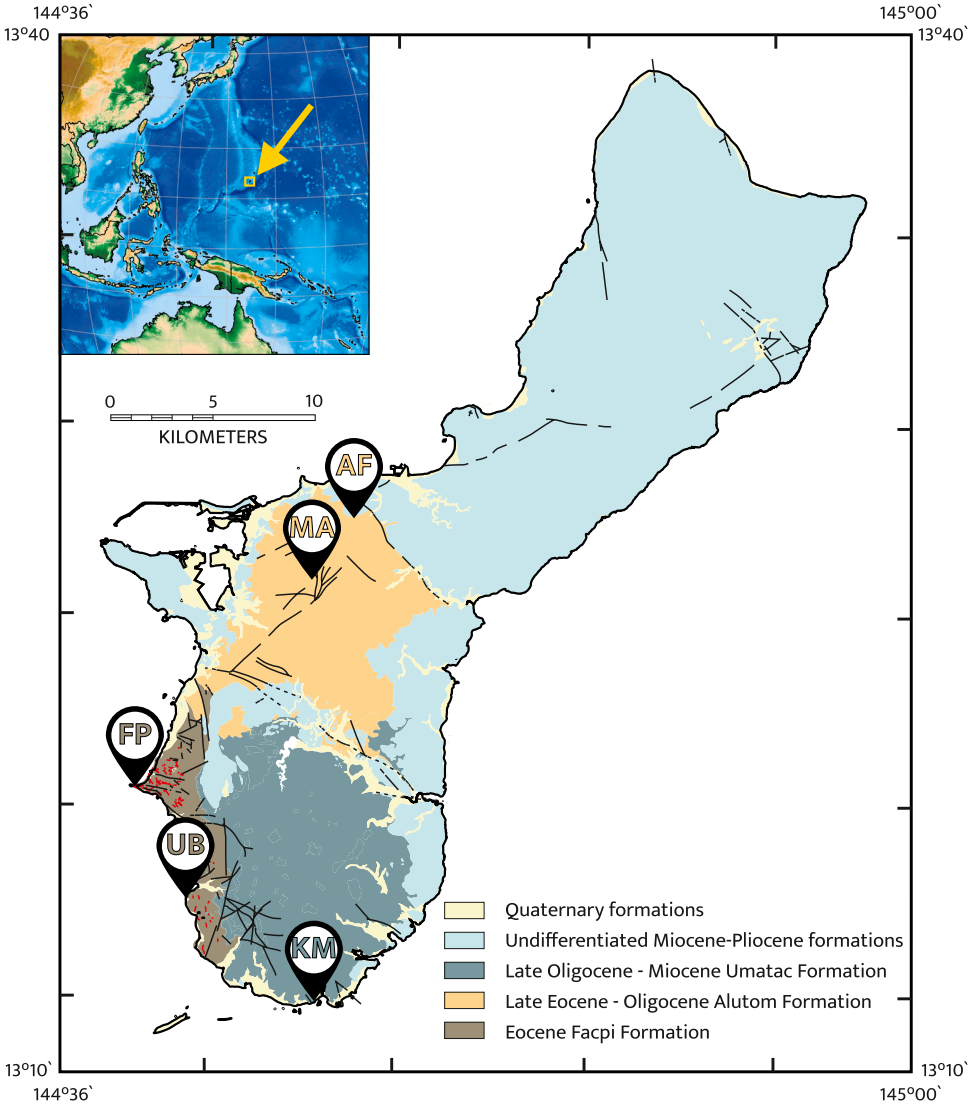

Fig. 2. Simplified geological map of Guam (based on Siegrist and Reagan, 2008), showing the different sampling locations indicated with the site names used in this study.

remnant arcs with intervening basins (e.g., Hickey-Vargas, 2005; Ishizuka et al., 2022; Hickey-Vargas et al., 2013; Morishita et al., 2018). Based on radiometrically dated dredged and drilled samples, it was interpreted that these basins opened in the Eocene, between c. 52 and 42 Ma (Hickey-Vargas, 1998; Ishizuka et al., 2013, 2018, 2022). The formation history of the different basins of the PSP thus indicates that the plate is a composite of about a dozen lithospheric fragments that formed at spreading centers in different orientations and at different times since ~54 Ma, within a Jurassic and Cretaceous lithosphere overlain by Cretaceous arc rocks.

Guam is the southernmost island exposed on the Mariana Ridge (Fig. 1). Together with the Northern Mariana Islands (Rota, Tinian, and Saipan), it forms the subaerially exposed forearc of the Mariana subduction zone. The currently active Mariana arc is located to the west and north of Guam and the Northern Mariana Islands. Guam exposes a stratigraphy spanning the Eocene to the Quaternary (Fig. 2). The northern half of Guam is dominated by Neogene limestone formations, which are also exposed in a smaller area in the southeast of the island (Fig. 2). The southern half of the island exposes Eocene to Miocene volcanics, volcaniclastic sediments, and minor limestones (Fig. 2). The oldest rocks exposed on Guam, dated to 43.8 ± 1.6 Ma using K—Ar whole-rock dating (Meijer et al., 1983), form the Eocene Facpi Formation, which comprises pillow basalts and andesite flows thought to have formed on the flanks of a strata-volcano (Reagan and Meijer, 1984; Siegrist et al., 2008). The Facpi Formation is exposed in the southwest of the island, with fresh outcrops along the coastline. Apart from a small eastward tilt, there is no coherent structure within the pillow basalts, but the orientation of (sub)vertical dikes is predominantly NW-SE to roughly *E*-W. The Facpi Formation is cut by steeply dipping normal faults with similar orientations as the dikes (Reagan and Meijer, 1984; Siegrist et al., 2008). Such normal faults do not occur in Miocene and younger formations, which suggests that they may have formed shortly after or during eruption of the Facpi Formation volcanics (Reagan and Meijer, 1984). Because of these faults, we interpret the 10–30° bedding tilts of the pillow basalts resulting from deformation.

The Eocene pillow basalts and dikes are overlain by Eocene-Oligocene sediments of the Alutom Formation, which comprises mostly volcaniclastics, including bedded breccias, conglomerates, turbiditic sandstones, and minor limestone (Reagan and Meijer, 1984; Siegrist et al., 2008). It is exposed in the northern part of the southern half of island, to the north of the Facpi Formation. The Alutom formation is late Eocene to earliest most Oligocene as shown by the occurrence of late Eocene foraminifera in its base section(Tracey Jr et al., 1964) and K—Ar whole rock ages between 35.6 ± 0.9 and 32.2 ± 1.0 Ma from its top (Meijer et al., 1983). Antiform and synform structures within the Alutom Formation are interpreted to be the result of volcano-tectonic collapse (Tracey Jr et al., 1964), possibly related to paleotopography during deposition.

The Alutom Formation is overlain by the Oligocene to Miocene Umatac Formation, which is exposed in the south of Guam. The oldest, Oligocene, rocks of this formation are interbedded limestones, sandy and tuffaceous limestones, sandstones, and conglomerates (Siegrist et al., 2008). The Miocene lithologies of the Umatac Formation consist of basaltic andesitic pillow lavas, volcanic sandstones, breccias, and conglomerates, and medium to coarse-grained andesite flows (Siegrist et al., 2008). The volcanic members of the Umatac Formation are highly weathered and only sporadically exposed. Bedding dips are mostly subhorizontal, although some steeper dips up to 35° have been recorded in the west, where the Umatac Formation is in direct structural contact with the Facpi Formation (Siegrist et al., 2008). As most of the Neogene formations have (sub)horizontal bedding planes, we interpret the steeper bedding dips in the west as related to paleotopography of the eroded pillow basalts on top of which the sediments were deposited and not as the result of deformation. As our samples were taken from a location with sub-horizontal bedding planes, this interpretation does not influence our paleomagnetic results.

3. Sampling and analytical methods

Paleomagnetic samples with a standard diameter of 25 mm were collected with a water-cooled, petrol-powered drill. The orientation of the samples was measured using a magnetic compass with an inclinometer attached. We collected samples from six localities on the island of Guam from volcanic and sedimentary rocks. We collected a single core per basalt pillow or per sedimentary bed to optimize the chance of sampling individual spot readings of the paleomagnetic field with each core, following sampling procedures for paleomagnetic poles recommended by Gerritsen et al. (2022).

We collected samples from two localities in the Eocene Facpi Formation, from two localities in the Eocene-Oligocene Alutom Formation, and from two localities in the Miocene Umatac Formation (Figs. 2 and 3). We collected samples from pillow basalts and lava flows at Facpi Point (FP1 and FP2; 63 samples) and Umatac Bay (UB; 34 samples). From the Eocene-Oligocene Alutom formation we collected samples from fine to coarse-grained turbiditic sandstones with volcanic detrital material and volcanic ash deposits at Mount Alutom (MA; 71 samples) and the Fonte River (AF; 64 samples). Collecting samples from Miocene rocks was complicated, as Miocene volcanic and volcaniclastic rocks exposed in Guam are highly weathered and only sporadically exposed, while Miocene limestones are often recrystallized. We collected 40 samples from coarse volcaniclastics of the Umatac Formation, at two relatively small road-sections along Highway 4 in the southernmost part of the island (KM1 and KM2 samples).

We carried out the paleomagnetic measurements at the paleomagnetic laboratory Fort Hoofddijk, Utrecht University (Utrecht, The Netherlands). Samples were either demagnetized using stepwise alternating field (AF) demagnetization in a robotized setup (Mullender et al., 2016) or stepwise thermal (TH) demagnetization. The magnetization was measured on a 2G DC-SQUID magnetometer. Throughout the demagnetization process, samples were kept in a magnetically shielded room.

Sample interpretation and statistical analysis was done using the online portal Paleomagnetism.org (Koymans et al., 2016, 2020). All our data are provided in the supplementary information and will be made available in the Paleomagnetism.org database (Koymans et al., 2020) as well as the MagIC database (Jarboe et al., 2012). Demagnetization diagrams were plotted as orthogonal vector diagrams (Zijderveld, 1967) and principal component analysis was used to the determine the characteristic remanent magnetizations (ChRM) component (Kirschvink, 1980). We used Fisher (1953) statistics on virtual geomagnetic poles following statistical procedures described in Deenen et al. (2011) to calculate site mean directions.

Thermomagnetic analyses were done with a modified horizontal translation Curie balance (Mullender et al., 1993) on selected samples from each locality to constrain the interpretation of the NRM components. The analysis was carried out in air and involved stepwise heating to 700 °C with intervened cooling to be able to discern potential thermochemical alteration due to the heating of the samples. The temperature sequence is as follows for most lithologies (in a cycling field between 200 and 300 mT): room temperature 150C° – 70 °C – 250 °C – 150 °C – 350 °C – 250 °C – 450 °C – 350 °C – 520 °C – 420 °C – 620 °C – 500 °C – 700 °C – room temperature. Where deemed appropriate the 150 °C segment with corresponding cooling to 70 °C was omitted. Curie temperatures are determined with the two-tangent method (Grommé et al., 1969). Each ChRM is interpreted with a minimum of four consecutive demagnetization steps. AF demagnetization steps affected by gyroremanent magnetization (Dankers and Zijderveld, 1981) were not used for ChRM interpretation. Where two components unblocked simultaneously and decay did not trend towards the origin, we used great circle interpretation (McFadden and McElhinny, 1988). In general, we interpreted ChRM directions without forcing the component through the origin, unless demagnetization behavior was noisy. We did not apply a maximum angular deviation cut-off, because Gerritsen et al. (2022)

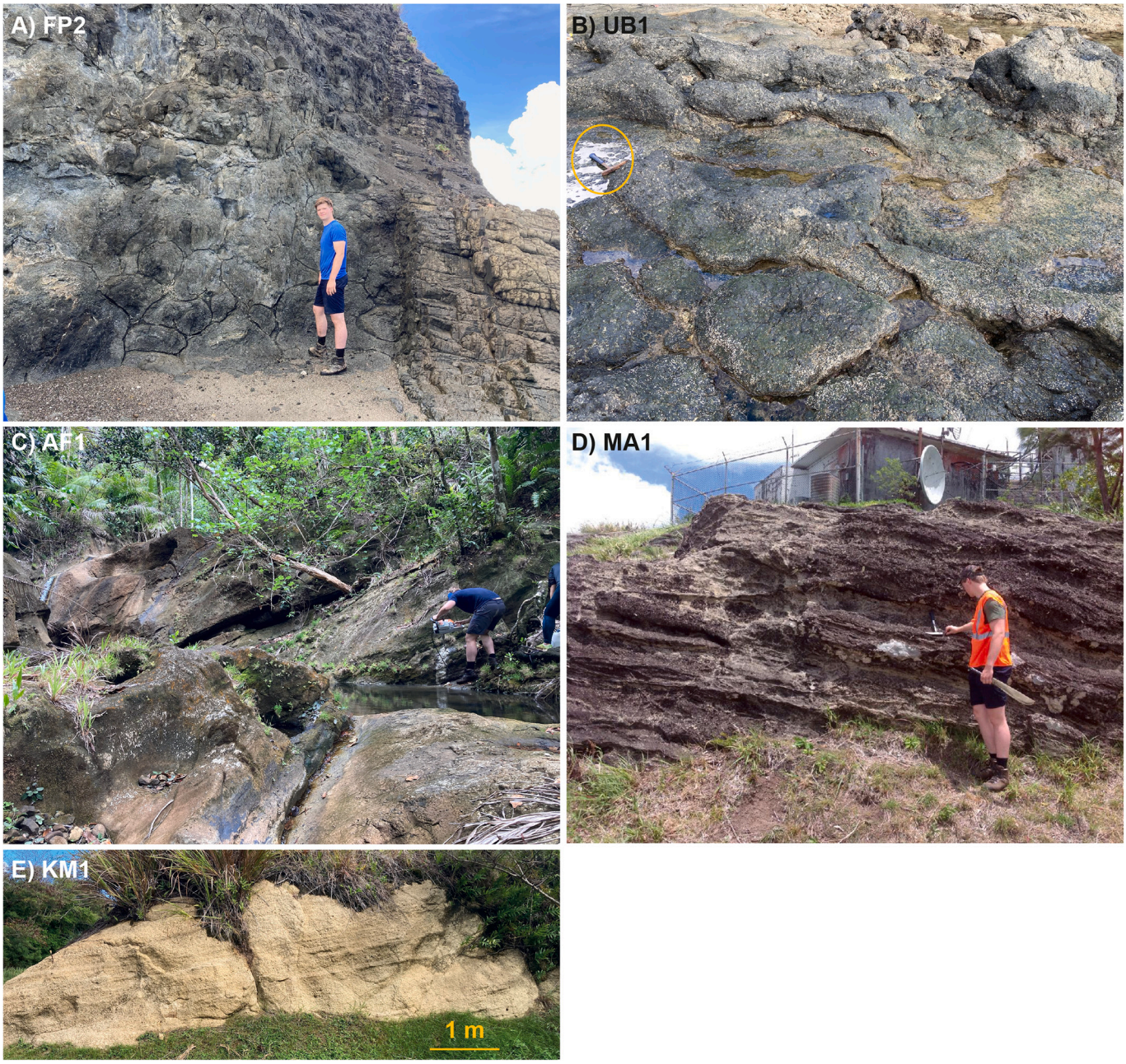

Fig. 3. Field photos of the different sampling locations. A and B) Pillow basalts and cross-cutting dike of the Eocene Facpi Formation; C and D) Volcaniclastics of the Oligocene Alutom Formation. E) Coarse pyroclastics from the Miocene Umatac Formation.

showed that this makes no difference for the precision or position of the final paleomagnetic pole, but we note that the widely-used MAD-cutoff of 15° would not have eliminated data. Finally, we applied a 45° cutoff (Johnson et al., 2008) to eliminate outliers, but this omitted <5% of the data.

4. Results and interpretation

4.1. Thermomagnetic results

The Eocene Facpi Formation pillow lavas (FP2.8 and UB1.1, ~0.5–0.6 Am^2/kg) are strongly magnetic, as expected for basaltic lavas (Fig. 4a-b). On heating in air, they oxidize to a variable extent. Barely or no oxy-exsolution is observed; it would be manifested by a corresponding cooling segment above the previous heating segment pointing towards formation of iron-richer titanomagnetite. FP2.8 shows two Curie temperatures, at ~470 °C and ~560 °C indicating titanomagnetite with a variable amount of Ti substitution. On heating to 700 °C, oxidation to less magnetic material, presumably hematite, is noted because the final cooling curve is below the heating segments. UB1.1only shows the higher Curie temperature, at ~560–570 °C indicating a very low level of Ti substitution. The Oligocene rocks of the Alutom Formation (~0.1 to 0.3 Am^2/kg; MA1.20, MA1.69; AF1.12; Fig. 4c-e) are less magnetic than the Eocene rocks. AF1.12 is essentially reversible up to 520 °C with only minute oxidation. Curie temperature is estimated at ~500–520 °C. Some oxy-exsolution appears in the next heating segment (and rises the Curie temperature). On further heating to 700 °C oxidation to less magnetic material is noted (Curie temperature remains at 500–520 °C). MA1.20 shows prominent oxy-exsolution across a large temperature interval: already after heating to 350 °C the behavior is visible which makes determination of the original Curie temperature tedious. MA1.69 is the weakest Oligocene sample; it

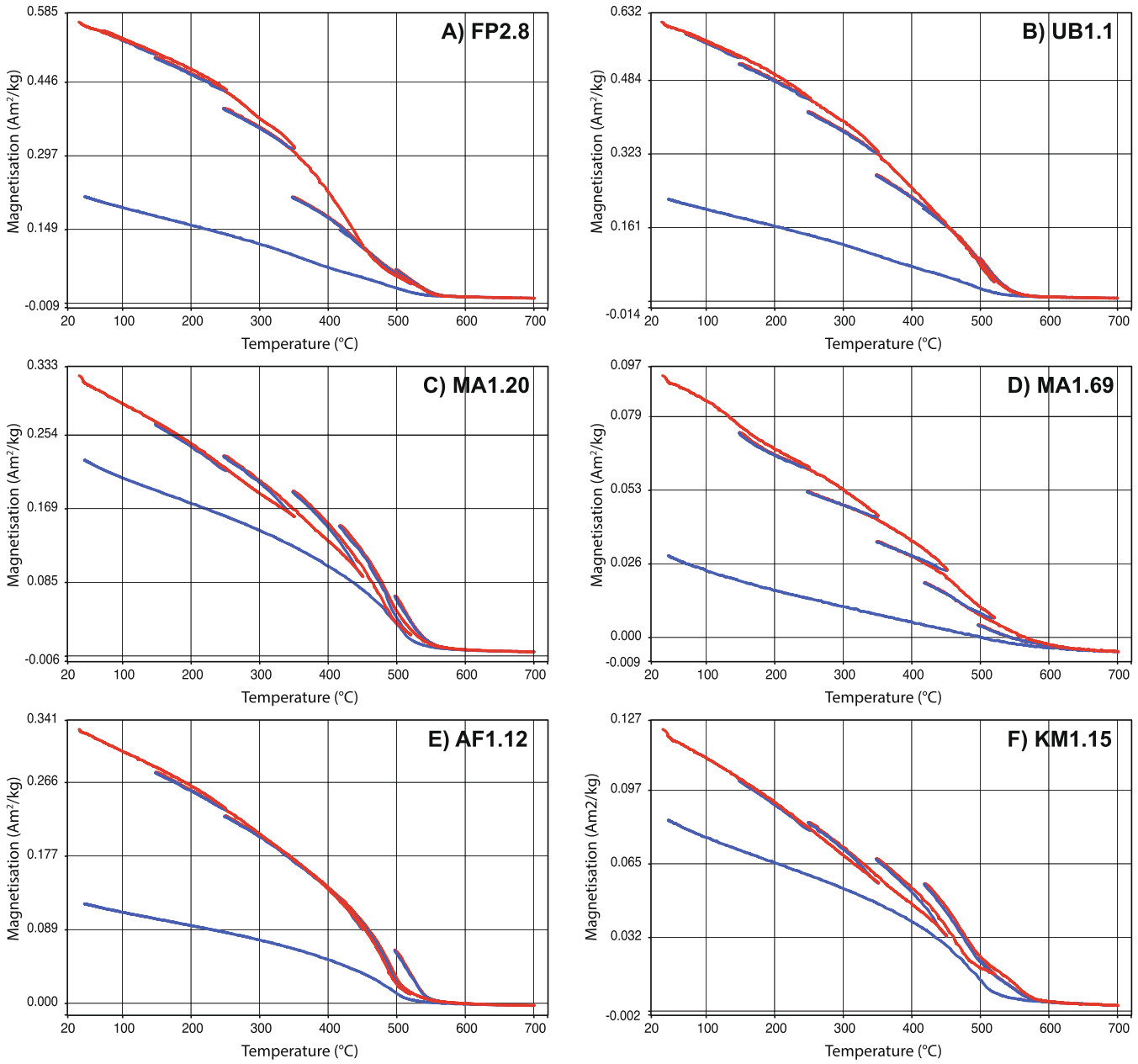

Fig. 4. Results of thermomagnetic analysis. Heating segments are in red, cooling segments are in blue. (For interpretation of the references to colour in this figure legend, the reader is referred to the web version of this article.)

behaves like FP2.8. The Miocene sample (KM1.15) is not that magnetic (~0.1 Am^2/kg) and shows prominent oxy-exsolution from 350 °C upward (Fig. 4). Oxidation at the highest temperature leads to a final cooling curve below the heating curves.

4.2. Paleomagnetic results

4.2.1. Facpi Formation

Paleomagnetic samples from the different sampling locations in the Facpi Formation basalts provided uniform demagnetization behavior. Thermal as well as AF demagnetization yielded small viscous overprints that were generally cleaned by 150 °C, occasionally up to 270 °C, or 10–15 mT, after which specimens decayed to the origin. Thermally demagnetized samples lost their signal after heating until ~510–580 °C, consistent with (titano-)magnetite as carrier, whereas AF demagnetization often started to deviate from the path towards the origin at fields of ~50 mT and higher. We interpret the latter behavior as gyroremanent magnetization (Dankers and Zijderveld, 1981), which is common for (titano-)magnetite-bearing basalts (e.g., van Hinsbergen et al., 2010). We interpreted the component decaying towards the origin as the ChRM, typically unblocking between ~180 and 580 °C, or between 15 and 50 mT (as at higher levels gyroremanent magnetization may interfere).

Thermal and AF demagnetization yielded similar directions (Fig. 5a, b). We corrected our paleomagnetic results for bedding strikes and dips of 349/20° E and 356/20° E in the FP and UB sites, respectively. We report both geographic (in-situ) and tectonic (tilt-corrected) results in Table 1, but limit our analysis to the tilt-corrected results, as these are interpreted as being representative of the paleomagnetic signal at the time of formation of the rock. The majority of samples yielded magnetic directions with shallow inclinations, and with northeasterly declinations (Fig. 5c, d). A small cluster of 7 stratigraphically consecutive samples in the UB locality has opposite polarity (Fig. 5a, b; Fig. 6b). We exclude outliers by applying a 45° cut-off, which eliminates a few directions. The

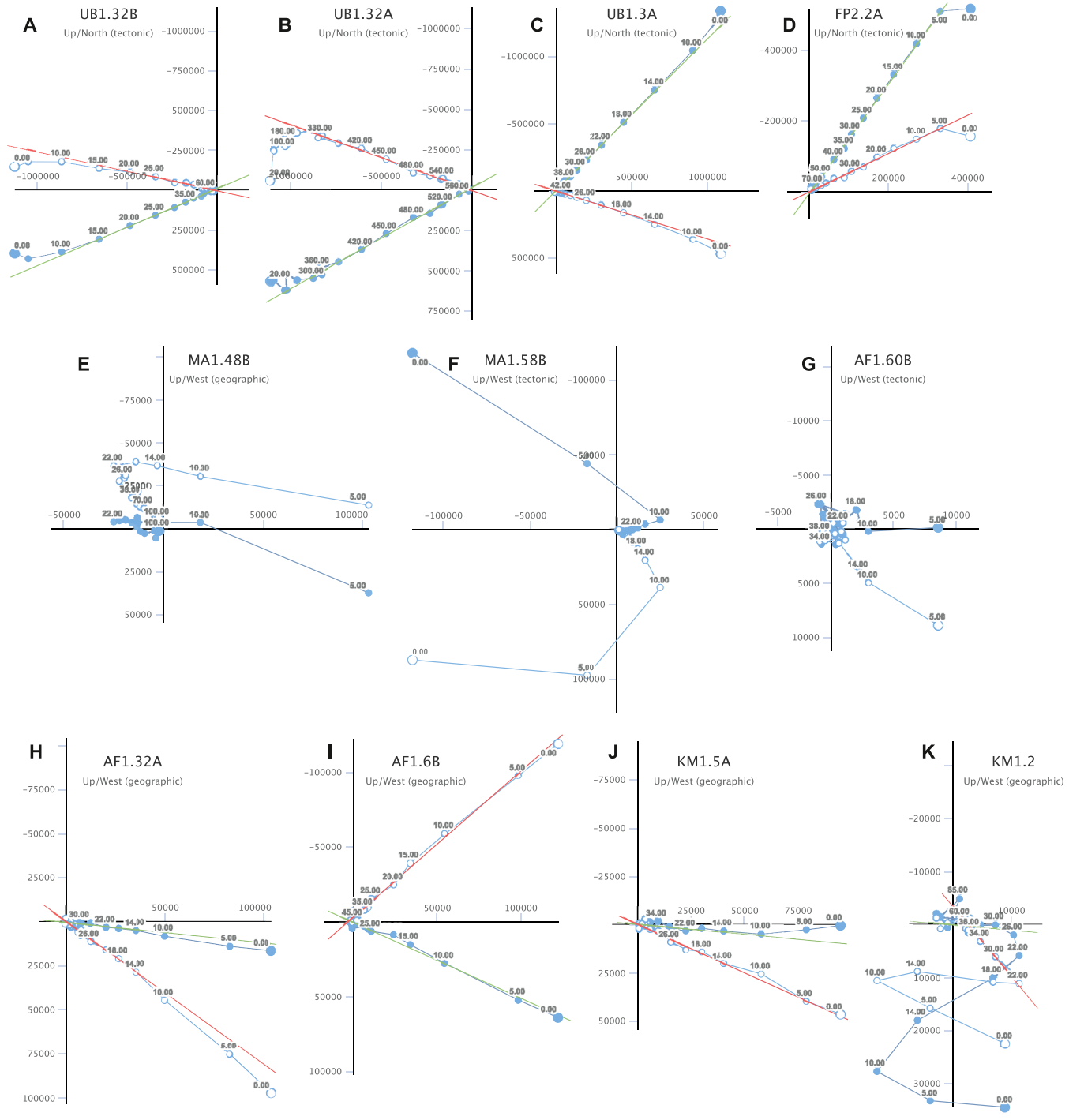

Fig. 5. Zijderveld demagnetization diagrams of selected samples. Closed circles for declination, open circles for inclination. Numbers along axes are intensities in μA/m.

opposite polarities ($N = 28$ vs $N = 7$) yield antipodal declinations, but the smaller dataset has a steeper inclination than the larger dataset (in geographic coordinates; Fig. 6b) such that a reversals test (of Tauxe, 2010) as implemented in Paleomagnetism.org (Koymans et al., 2016) is negative. Our interpretation is that the small dataset may not adequately represent the reversed magnetic field, possibly resulting from insufficient averaging of paleosecular variation (PSV). Nonetheless, we consider the presence of reversals in the sequence as a signal that the ChRM is primary. The FP sampling locations were cut by dikes with thicknesses up to ~5 m. To evaluate whether the intrusion of these dikes may have remagnetized the surrounding pillow lavas, we collected 5–8 samples each from one dike cutting FP1 and three dikes cutting FP2. These dikes yielded K-values of 17–130. The K-values (between 17 and 57) of three of the dikes are consistent with PSV-induced scatter (Deenen et al., 2011), suggesting that they cooled gradually, and each sample represents a spot reading of the field, while the K-value (130) of the fourth dike suggests rapid cooling, which means that this dike represents a single spot-reading. In addition, while the average directions of the dikes and the lavas are northeasterly, they are not identical to the clusters from the pillow lavas (Fig. 6a). The scatter within and difference between the average directions of the dikes and the pillow lavas is straightforwardly explained by the low number of samples underpinning

Table 1
Paleomagnetic results.

Geographic (in situ) coordinates															
Locality	Age	Latitude (°N)	Longitude (°E)	N	Ns	Dec (°)	Inc (°)	k	a95	K	A95	$A95_{Min}$	$A95_{Max}$	ΔDx (°)	ΔIx (°)	λ (°)
FP	Eocene	13.3419843	144.636729	79	73	37.05	7.65	9.15	5.81	14.72	4.48	2.16	5.49	4.49	8.83	3.84
UB	Eocene	13.29565	144.6597	38	36	73.52	3.94	15.9	6.18	23.7	5.01	2.86	8.58	5.01	9.99	1.97
AF	Oligocene	13.459	144.73102	121	113	352.17	23.04	35.49	2.26	47.52	1.95	1.81a	4.17	1.99	3.45	12.01
MA	Oligocene	13.43244	144.7129	79	69	9.98	18.08	13.9	4.75	18.52	4.08	2.21	5.69	4.13	7.57	9.27
KM	Miocene	13.249215	144.716595	46	36	355.67	21.36	9.4	8.24	15.3	6.31	2.86	8.58	6.43	11.37	11.06
Tectonic (tilt-corrected) coordinates																
Locality	Age	Latitude (°N)	Longitude (°E)	N	Ns	Dec (°)	Inc (°)	k	a95	K	A95	$A95_{Min}$	$A95_{Max}$	ΔDx (°)	ΔIx (°)	λ (°)
FP	Eocene	13.3419843	144.636729	79	72	37.26	−8.19	9.47	5.74	14.98	4.47	2.17	5.54	4.48	8.8	−4.12
UB	Eocene	13.29565	144.6597	38	35	71.92	−14.96	18.14	5.85	29.14	4.57	2.89	8.73	4.61	8.68	−7.61
AF	Oligocene	13.459	144.73102	121	113	335.05	40.45	23.14	2.82	24.13	2.76	1.81	4.17	3	3.78	23.09
MA	Oligocene	13.43244	144.7129	79	71	4.45	8.5	13.79	4.7	22.55	3.62	2.18	5.59	3.63	7.13	4.28
KM	Miocene	13.249215	144.716595	46	33	346.1	21.77	8.65	9.03	14.11	6.9	2.96	9.06	7.04	12.38	11.29

N: number of samples; Ns: Number of samples that are used for the analysis after 45° cut-off; Dec: Declination; Inc.: Inclination; ΔDx/ΔIx: uncertainty in declination/inclination; λ: paleolatitude.

these averages (see Vaes et al., 2022). These results therefore do not suggest that dike intrusion remagnetized the surrounding pillow lavas, but rather that the samples collected from the pillow lavas and dikes each may be considered a spot reading from the paleomagnetic field.

We computed a grand average for the FP locations and for the UB location (Fig. 6c; Table 1), which are located 6 km apart. The FP locations yielded a direction of Dec/Inc. = 37.3 ± 4.5°/−8.2 ± 8.8° ($N = 72$, K = 15.0, A95 = 4.5) and the UB location yielded a direction of Dec/Inc. = 71.9 ± 4.6°/−15.0 ± 8.7° ($N = 35$, K = 29.1, A95 = 4.6). Both pass the Deenen et al. (2011) criteria, suggesting that their data scatter can be straightforwardly explained by PSV alone. The inclinations of both localities are very similar (paleolatitudes of 4.1° and 7.6° N or S; Fig. 6c), but the declinations reveal a ~ 35° difference in vertical axis rotation. A southern hemisphere normal component would require clockwise rotations of 37° and 72° relative to the present-day GAD field, a northern hemisphere reversed component would require counterclockwise rotations of 147 and 108°, respectively. We consider the smaller rotations the most likely and use these in the data compilation.

4.2.2. *Alutom and umatac formations*

Demagnetization diagrams of the MA section display varying demagnetization behavior throughout the section that is characterized by consecutive samples with similar behavior that strongly differs from subsequent parts of the section. This is probably owing to the volcaniclastic nature of the section, whereby beds may represent volcanic events, as well as intra-volcanic sedimentary deposits. First, the magnetization intensity varies strongly, from several 10.000 to several million mA/m. Second, the magnetizations, typically showing decay towards the origin, display varying degrees of overprinting. South-directed (likely reverse) overprints occur on north-directed magnetizations and vice versa (Fig. 5e, f). These may represent recent overprints of a normal field over a primary reverse magnetization, but also an overprint induced by a volcanic episode during a reverse polarity state of the field over a primary normal magnetization. In addition, the presence of volcanic events is suggested by the tight clustering of directions of consecutive samples in the section. For example, samples MA1.50-MA1.56 show a tightly clustered reverse magnetization (k = 250, n = 7), an overlying sequence of MA1.58–1.66 yield a nearly antipodal direction with a k-value of 133 (n = 8) (Fig. 6d). Such tight clustering is much higher than may be expected from PSV (Deenen et al., 2011) and likely represent paleomagnetic spot readings recorded in discrete volcanic events.

When all dominant magnetizations, i.e., of the components that decay towards the origin, are combined into a single plot, it is evident that clusters of opposite polarity are present in the section, as well as a large cluster of data around the recent paleomagnetic field direction. We suspect that the magnetizations include recently remagnetized and primary magnetizations (Fig. 6d). Because we cannot establish with certainty per sample which directions are overprints and which are primary, and because of the evidence that sets of primary directions may represent single spot readings of the field, we do not consider the directions we determined as a reliable indicator of the paleomagnetic field. We refrain from using the paleomagnetic data from MA for further analysis. Samples of section AF typically display gradual decay towards the origin defining single components with little overprint. In some cases, the magnetization is only carried by carriers that lost their magnetization by ~20 mT, after which only erratic behavior remains (Fig. 5g). We interpret these samples as only carrying a recent overprint. The remainder of samples demagnetized typically until 50–60 mT or ~ 270 and 500 °C, after which only erratic behavior of low-intensity magnetization remained (Fig. 5h, i). Interpreting the components that decay towards the origin as the ChRM leads to a tight cluster of directions with D = 352.2 ± 2.0; I = 23.0 ± 3.5; K = 47.5, A95 = 2.0, N = 113. The clustering of the data is tight (Fig. 6e) but may still be explained by PSV ($A95_{min}$ sensu Deenen et al. (2011) for N = 113 is 1.8). Because the bedding is changing orientation throughout the section,

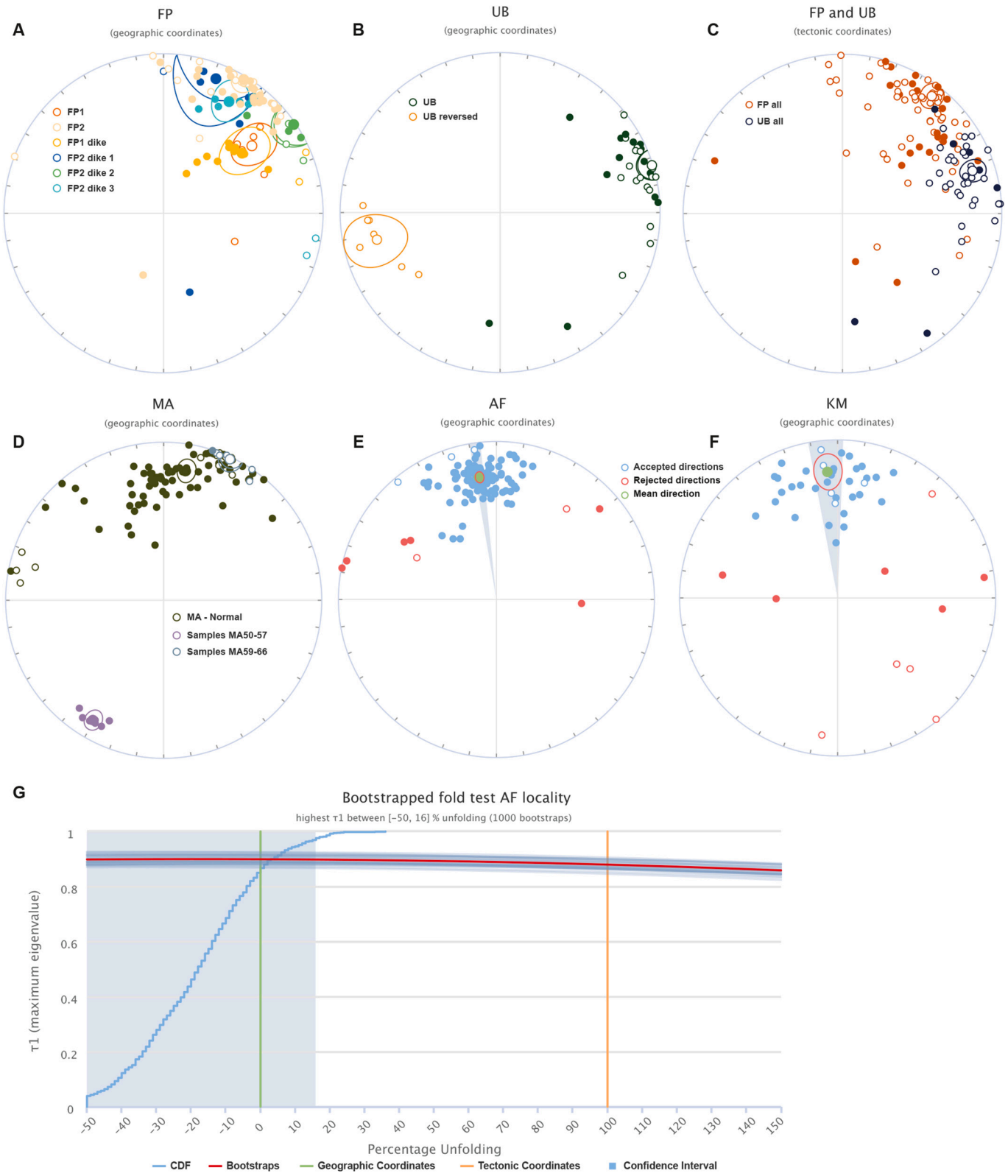

Fig. 6. Paleomagnetic results from the different sections. A-F) Paleomagnetic directions and means of the different sampled sections. Open (closed) symbols are up (down) directions. G) Fold test of the AF locality.

varying in dip by ~25°, we performed a fold test, which is clearly negative (Fig. 6g). The paleolatitude computed from the paleomagnetic direction in geographic coordinates is ~12°, which corresponds to the latitude of the sampling location. This, combined with the solely normal magnetization leads us to interpret the magnetization of section AF as a recent overprint, whereby the small counterclockwise rotation may reflect the effects of e.g., land sliding or otherwise minor, recent deformation.

Finally, the Miocene sites of KM display demagnetization behavior that is similar to that of site AF. A minor viscous overprint is typically

demagnetized by 10 mT (Fig. 5j), although non-systematic overprint directions are occasionally demagnetized until ~20 mT (Fig. 5k), after which demagnetization decays to the origin until ~50 mT. At higher demagnetization steps, decay becomes noisy. Thermal demagnetization diagrams are incomplete because the loose samples disintegrated during thermal demagnetization. Interpreting the magnetizations that decay towards the origin as the ChRM leads to a clustering of normal polarity, north-directed directions. The average direction is D = 355.7 ± 6.4°, I = 21.4 ± 11.4°, K = 15.3, A95 = 6.3, N = 36 (Fig. 6f; Table 1). This is an insignificant difference with the recent GAD direction predicted for the sampling location. A fold test is permitted because there is bedding orientation variation. This fold test gives optimal clustering at <0% unfolding, which may suggest that some folding of an originally undulating sedimentary cover occurred prior to magnetization. The cluster of paleomagnetic directions may in principle be explained by PSV ($A95_{min, max}$ = 2.9, 8.6 sensu Deenen et al., 2011). Nonetheless, the insignificant difference between the average direction in geographic coordinates with the recent field, combined with the negative fold test leads us to not consider this result as a primary magnetization from which we may infer tectonic motion of Guam since the Miocene. Combined, we do not interpret the samples from the two Oligocene sections or the Miocene sites to carry a resolvable primary magnetization, and where it may, it does not represent a long-term GAD direction with representative PSV scatter.

5. Paleomagnetic data compilation

We compiled published paleomagnetic data from the PSP, to which we added our two sites from the Eocene Facpi Formation of Guam that were interpreted as primary directions. The database contains data from boreholes that drilled into igneous basement, and from field localities in the Philippines and the northern Maluku islands, from Palau, Guam, the Northern Mariana, and Ogasawara islands. We compiled site-level data as originally published, whereby we followed the authors' interpretations about magnetic field polarity and whether bedding tilt corrections were applicable. We subsequently calculated mean paleomagnetic directions from collections of similar age and locations, using the online portal Paleomagnetism.org (Koymans et al., 2016, 2020), whereby we assumed that each reported direction, i.e., a lava site, represents a spot reading of the magnetic field, regardless of its k-value. If an antipodal paleomagnetic direction is present within a locality, we flipped the polarity and combined the data into one collection before calculating the locality mean. Before calculation of the paleomagnetic mean direction, we excluded sites if they were rejected by the original authors. In addition, we did not calculate means for localities with fewer than 4 sites. Our calculated means may differ from the originally published mean direction, for example when the authors mixed sedimentary sites with igneous sites, which we kept separate. We applied a 45° cut-off to exclude outliers and transitional directions before recalculation of mean directions. After recalculation of mean paleomagnetic directions, we excluded localities with K values (Fisher (1953) precision parameters on poles) below 10 (following Meert et al., 2020) or when means yielded an A95 outside the A95min-max confidence envelope of Deenen et al. (2011). Our recalculated means are provided in Table 2, while the site-level compilation is provided in Supplementary Table S1. A total of 20 paleomagnetic poles in our PSP compilation passed our quality criteria, obtained from lava flows, pillows, or dikes, as well as 7 paleolatitudes obtained from boreholes.

Paleomagnetic data obtained from sedimentary rocks were not added to the compilation, because it is unclear whether the reported sites represent spot-readings of the field or whether a site adequately averages PSV. In addition, the number of samples collected at the sedimentary localities is insufficient (i.e., <80–100, see Tauxe and Kent, 2004; Vaes et al., 2021) to properly apply the E/I inclination shallowing correction (Tauxe and Kent, 2004), prohibiting using these data to assess paleolatitudinal motion. In a few cases, paleomagnetic datasets obtained

Table 2
Paleomagnetic data compilation (field sites only).

Location	Age (Ma)	Lat (°N)	Lon (°E)	N	Ns	Dec (°)	Inc (°)	k	a95	K	A95	$A95_{Min}$	$A95_{Max}$	ΔDx (°)	ΔIx (°)	λ (°)	Reference
Central Cordillera	2.6 ± 2.6	16.672	120.822	6	6	349.88	30.59	23.71	14.04	20.87	15.01	5.86	26.52	15.67	24.19	16.46	Queaño et al. (2007)
Batangas	7.0 ± 0.8	13.7	121.2	6	6	318.28	35.35	39.34	10.81	38.76	10.9	5.86	26.52	11.57	16.32	19.53	Fuller et al. (1991)
Central Cordillera	10.2 ± 4.9	18.062	120.998	8	7	274.88	20.65	23.71	12.65	29.32	11.33	5.51	24.07	11.54	20.55	10.67	Queaño et al. (2007)
Obi*	11 ± 1	−1.58	127.83	4	4	14.17	−41.89	452.72	4.32	368.69	4.79	6.89	34.24	5.25	6.38	−24.15	(Ali and Hall, 1995)
Obi	11.3 ± 3.0	−1.52	127.95	9	9	327.78	−25.91	57.2	6.87	103.87	5.08	4.98	20.54	5.22	8.7	−13.65	(Ali and Hall, 1995)
Saipan	12 ± 3	15.13	145.71	5	5	28.76	31.87	57.07	10.21	79.36	8.64	6.3	29.75	9.05	13.67	17.27	Haston and Fuller (1991)
Central Cordillera	14.2 ± 8.9	16.45	120.8	4	4	315.49	7.73	39.8	14.74	50.46	13.06	6.89	34.24	13.09	25.76	3.88	Fuller et al. (1991)
Sierra Madre	16.04 ± 4.41	15.368	121.24	5	5	297.55	19.14	17.96	18.55	18.31	18.37	6.3	29.75	18.65	33.77	9.85	Queaño et al. (2007)
Palau	20.1 ± 0.5	7.37	134.52	5	5	54.48	3.48	20.31	17.39	32.69	13.58	6.3	29.75	13.59	27.09	1.74	Haston et al. (1988)
Guam	28.5 ± 5.5	13.45	144.7	4	4	57.67	10.73	61.13	11.85	98.58	9.3	6.89	34.24	9.34	18.12	5.41	Haston and Fuller (1991)
Kasiruta	32.3 ± 3.0	1.18	128.31	9	9	40.49	−24.68	27.64	9.97	29.61	9.62	4.98	20.54	9.87	16.72	−12.94	Hall et al. (1995b)
Saipan	35.8 ± 1.9	15.23	145.8	12	11	42.09	−8.68	13.2	13.05	21.31	10.12	4.6	18.1	10.15	19.9	−4.37	Haston and Fuller (1991)
Guam	43.8 ± 2.6	13.296	144.660	38	35	71.92	−14.96	18.14	5.85	29.14	4.57	2.89	8.73	4.61	8.68	−7.61	This study
Guam	43.8 ± 2.6	13.342	144.637	79	72	37.26	−8.19	9.47	5.74	14.98	4.47	2.17	5.54	4.48	8.8	−4.12	This study
Hahajima	45 ± 7	27.08	142.16	7	7	32.69	2.86	11.24	18.82	19.43	14.04	5.51	24.07	14.05	28.03	1.43	Kodama et al. (1983)
Sierra Madre	45 ± 11	17.216	122.313	7	7	230.18	−2.7	19.93	13.86	30.41	11.12	5.51	24.07	11.13	22.21	−1.35	Queaño et al. (2007)
Anijima	45 ± 7	27.12	142.21	16	14	86.84	9.04	7.41	15.66	14.22	10.92	4.18	15.55	10.96	21.44	4.55	Keating et al. (1983)
Chichijima	45 ± 7	27.08	142.21	27	25	104.96	9.98	6.77	12.04	10.54	9.37	3.31	10.79	9.4	18.31	5.03	Kodama et al. (1983)
Zambales	46.4 ± 5.3	15.657	120.057	6	6	288.7	−0.1	17.64	16.4	49.39	9.63	5.86	26.52	9.63	19.25	−0.05	Fuller et al. (1989)
Zambales	46.4 ± 5.3	15.56	120.08	13	13	235.29	−1.96	18.85	9.8	36.67	6.94	4.3	16.29	6.94	13.86	−0.98	Fuller et al. (1989)
*Central Cordillera**	67 ± 33	17.17	121.06	5	5	159.26	−12.47	162.46	6.02	400.54	3.83	6.3	29.75	3.85	7.39	−6.31	Queaño et al. (2009)
Samar	99.0 ± 3.9	11.1	125.25	13	13	341.6	−26.6	14.69	11.19	25.88	8.3	4.3	16.29	8.56	14.11	−14.06	Balmater et al. (2015)

N: number of samples; Ns: Number of samples that are used for the analysis after 45° cut-off; Dec: Declination; Inc.: Inclination; ΔDx/ΔIx: uncertainty in declination/inclination; λ: paleolatitude.
* A95 outside of Deenen et al. (2011) confidence ellipse.

from sedimentary rocks of boreholes contain sufficient samples to correct for inclination shallowing, especially large magnetostratigraphic sections, but individual directional data is needed for the E/I correction. Also, these borehole data do not contain declination data because they are not azimuthally oriented. Recently, declination data from a borehole in the PSP were obtained from an oriented core (Yamazaki et al., 2021). However, the uncertainty on these data remains unknown and with their limited number of samples (13 samples from each of two cores of c. 30 cm), the data cannot be used for paleolatitude constraints. For these reasons, all sedimentary data are excluded from our compilation.

6. Discussion

Determining the vertical axis rotation of the PSP using paleomagnetic data is not straightforward. First, datasets are typically small ($N < 10$) and the dispersion of such datasets around the true pole is often larger than suggested by their A95 error margins, and the reliability varies with N (Vaes et al., 2022). Both easterly and westerly declinations have been obtained, generally westerly in the northern Philippines, and generally easterly on the islands in the south and east of the plate (Fig. 7). However, which of these declinations, if any, are representative for the rotation history of the plate as a whole is difficult to assess given that all locations come from its deformed plate margins. The Philippine Mobile Belt, which comprises PSP's western boundary, is cross-cut by major left-lateral strike slip faults, including the 1200 km long Philippine Fault (Aurelio et al., 1991), which are bound to induce local block rotations (Queaño et al., 2007, 2009). Similarly, the northern Maluku islands, including Halmahera and Obi, are in the south crosscut by the Sorong Fault system and are in an upper plate position relative to the Halmahera trench (Fig. 7). This position in a tectonically active region increases the likelihood of local block rotations, as shown by the strongly varying paleomagnetic declinations (Ali and Hall, 1995; Hall et al., 1995a). Moreover, a problem with paleomagnetic data from igneous rocks, often from stratovolcanoes of arcs, is that structural control on bedding tilt is generally poor, and the effect of small tectonic tilts on large primary bedding dips cannot be seen in the field.

Whether local deformation played a role in the paleomagnetic data obtained from the islands along the eastern margin of the PSP was poorly defined. The declination difference of 35° that we obtained from two Eocene localities in Guam shows that local block rotations also played a role in the forearc of the Mariana Trench. All paleomagnetic poles from the eastern PSP margin that pass our quality criteria have been interpreted as an easterly deflection of the magnetic field (Fig. 7). These data may reflect a clockwise rotation of the entire PSP, albeit significantly less than the widely assumed 90° (Haston and Fuller, 1991; Hall et al., 1995a; Seton et al., 2012; Liu et al., 2023). However, due to their sub-equatorial paleolatitude, the polarity of these data, and hence the sense of rotation, is not well known (Kodama et al., 1983; Haston and Fuller, 1991). Moreover, most reliable paleomagnetic poles obtained from the eastern margin of the plate were obtained from the southern forearc regions, i.e., Saipan, Guam, and Palau. The curved shape of the Mariana and Palau arcs may result from local rotations during opening of back-arc basins, which makes interpreting these data as unequivocal evidence of plate-wide rotations difficult to defend.

Despite the limited number and the questionable use of paleomagnetic data to infer whole-PSP motion, many plate motion models suggest

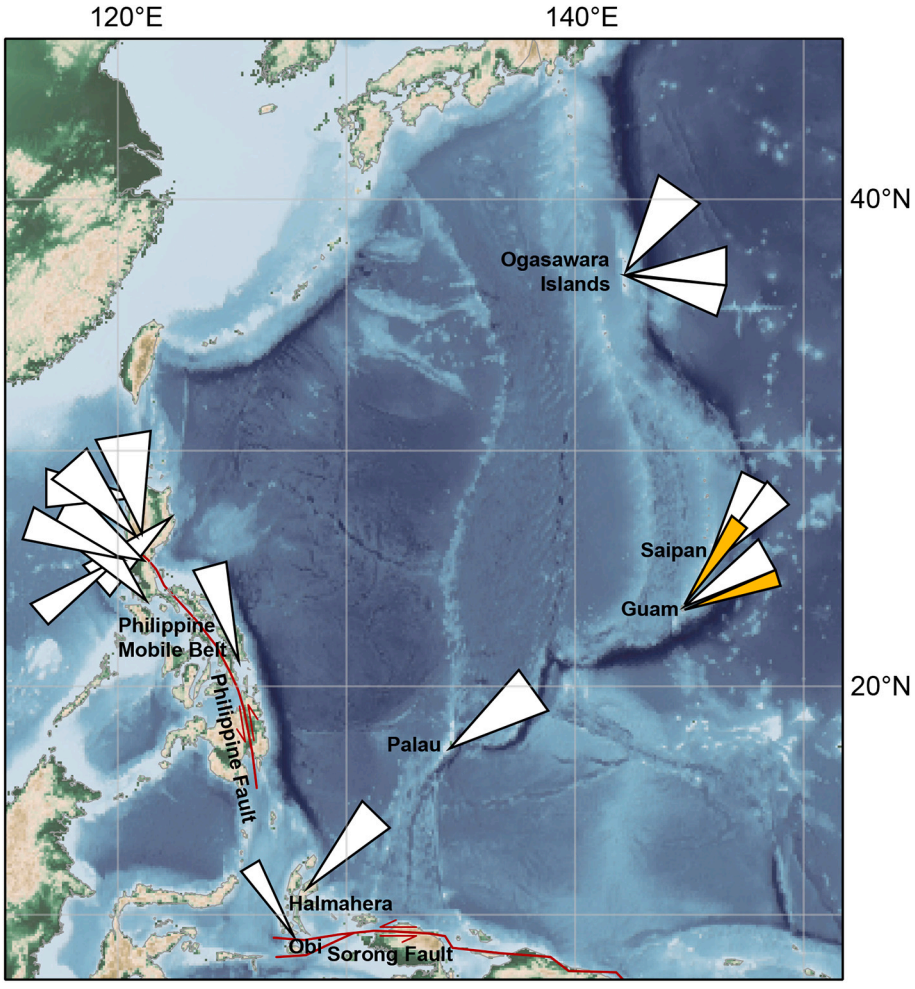

Fig. 7. Map of the Philippine Sea Plate showing declinations in our paleomagnetic data compilation with A95 confidence parachutes. White parachutes mark previously published paleomagnetic data, yellow parachutes mark our new paleomagnetic data from Guam. Base map is ETOPO, 2022 15 Arc-Second Global Relief Model (NOAA National Centers for Environmental Information, 2022). (For interpretation of the references to colour in this figure legend, the reader is referred to the web version of this article.)

that the Philippine Sea Plate underwent a large-scale clockwise rotation, of about 90° (e.g., Hall et al., 1995a; Yamazaki et al., 2010; Seton et al., 2012; Wu et al., 2016; Liu et al., 2023). This idea was originally proposed based on the first paleomagnetic results from the Philippine Sea Plate (Keating and Helsley, 1985; Haston et al., 1988; Haston and Fuller, 1991), although some authors suspected that local vertical-axis rotations resulting from arc bending or forearc rotation were actually more realistic (McCabe and Uyeda, 1983; Keating et al., 1983; Kodama et al., 1983; Seno and Maruyama, 1984; Keating and Helsley, 1985). Subsequently, based on data from the northern Maluku islands, Hall et al. (1995a) suggested that the PSP underwent a 50° clockwise rotation between 50 and 40 Ma, no rotation between 40 and 25 Ma, and an additional 35° clockwise rotation between 25 and 5 Ma. More recent studies compiled paleomagnetic data (e.g., Wu et al., 2016), and some studies questioned the validity of some of the existing paleomagnetic data, including the possibility of local block rotations and raised the issue whether some localities, such as Halmahera, have been part of the PSP throughout the Cenozoic (Xu et al., 2014; Zahirovic et al., 2014; Wu et al., 2016). However, the quality of the existing data was never assessed in detail using recent quality criteria (Meert et al., 2020; Vaes et al., 2021; Gerritsen et al., 2022) and it was thus never quantitively assessed whether the existing paleomagnetic data are reliable to infer PSP motions. Therefore, despite the suspicion of compromised data, the idea of a large-scale clockwise rotation of the entire PSP plate is still widely used, and recent plate tectonic reconstructions often assumed clockwise rotations of up to 90°, citing paleomagnetic data (Seton et al., 2012; Wu et al., 2016; Liu et al., 2023).

Based on our new compilation of PSP paleomagnetic data, however, we find that the paleomagnetic database is not of sufficient quality to form a basis to invoke rotation of the entire plate. Notably, the quality criteria that we used for the compilation in this paper are loose compared to those of Meert et al. (2020). If we were to apply the criterion of Meert et al. (2020) that each locality should include at least 8 sites (spot-readings), only nine paleomagnetic results would pass, of which two are from this study, and our data reveal strong local rotations. Applying additional criteria of Meert et al. (2020), one of the nine remaining poles would be discarded because of its K-value >70, even though it passes the Deenen et al. (2011) criteria, and our two new poles would be discarded because we did not take a minimum of 3 samples per individual lava flow (even though doing so cannot be demonstrated to significantly change the precision or position of paleomagnetic poles (Gerritsen et al., 2022), which is why we focused on maximizing the number of spot readings). This would leave only six datapoints; two from the Philippine Mobile Belt, with strongly varying declinations demonstrating that local block rotations must have occurred (e.g., Queaño et al., 2007, 2009), and two from the North Maluku islands that are also in the deformed plate margin (e.g., Wu et al., 2016; Pubellier et al., 1999). Hence, the declinations of the PSP paleomagnetic database should not be used as basis for plate reconstructions.

This does not mean, of course, that paleomagnetic data exclude such rotations. It may well be that the entire PSP underwent regional vertical axis rotation. However, this rotation should follow from the kinematic reconstruction of the region and existing paleomagnetic data should not be used as input for such reconstructions. The paleomagnetic data obtained by Yamazaki et al. (2021) from oriented drill-cores from the PSP's interior may be the first declination data that are representative for a vertical-axis rotation of the entire PSP. These data suggest a ~ 50° clockwise rotation of the PSP since the mid-Oligocene (c. 28 Ma), which is distinctly less than the ~90° rotation that is incorporated in many PSP models. However, the small number of samples and the unknown uncertainty in declination, makes the data insufficient as a basis for kinematic reconstruction. Yamazaki et al. (2021)'s study, however, shows that the large paleomagnetic datasets from the drill cores of the plate interior may provide a promising avenue towards obtaining quantitative constraints on plate rotation, but it is currently unknown what the uncertainty associated with the core-rotation correction is, and how this propagates into the final declination estimate. However, the mostly sedimentary rocks from the drill cores need to be corrected for inclination shallowing correction before also the inclination data can also be used for plate reconstruction.

We may use the data from igneous rocks in our compilation to infer PSP's paleolatitudinal motion. To this end, we compare the net paleolatitudinal displacements of the sampling sites between their moment of formation and the present, in a 'Huatung Basin-fixed' frame. We chose the Huatung Basin because it is the oldest oceanic lithosphere of the PSP and therefore exists throughout the reconstructed period. We reconstructed opening of PSP's oceanic basins using the available magnetic anomaly data (Hilde and Chao-Shing, 1984; Deschamps and Lallemand, 2002; Yamazaki et al., 2003; Sdrolias et al., 2004), making a 'Philippine plate motion chain'. The root of this plate motion chain is the Huatung Basin, and all motions are reconstructed relative to this microplate. We subsequently infer the paleolatitudinal correction that the Huatung Basin needs to get to fit with the paleomagnetic data in our compilation. The paleolatitude results show that a northward motion of about 15° since 45 Ma (Fig. 8) is suggested by the paleolatitude data, although the scatter is quite large. Our ~15° estimate is ~5° less northward motion than previous estimates (Louden, 1977; Kinoshita, 1980; Hall et al., 1995b; Haston and Fuller, 1991; Queaño et al., 2007; Yamazaki et al., 2010). The c. 5° difference may be explained by the fact that most boreholes are from the northern half of the PSP (Fig. 1), which underwent additional northward motion accommodated by spreading in the West Philippine Basin (Hilde and Chao-Shing, 1984). Without correction for the opening of the West Philippine Basin, a larger northward motion of up to 7° of the entire plate would be inferred. We find no systematic trend between paleolatitudinal mismatches and sampling location that would unequivocally demonstrate a large-scale whole-plate vertical axis rotation. The single mid-Cretaceous pole obtained from the Philippine Mobile Belt (Balmater et al., 2015) suggests that the latitudinal position of the 'proto-PSP' at that time was about 10° south of its mid-Eocene position (Table 2), although more paleomagnetic data is needed to confidently determine the pre-Eocene latitudinal evolution of the proto-PSP. This single pole, however, suggests that the Philippine arcs cannot have been part of the Izanagi Plate, which was moving considerably faster to the north (Seton et al., 2012; Boschman et al., 2021; Wu et al., 2022). Instead, the proto-PSP formed part of a plate that was located in the junction region between the Tethyan and Panthalassa realms.

Finally, improved constraints on PSP motion may be obtained from the available drill-cores of the PSP, especially magnetostratigraphic data that contain large sample sets. These data are currently only useful for assessing general trends in paleolatitude evolution, but future efforts to correct for inclination shallowing may significantly improve their value. Subsequently, if the paleolatitude of different drill-cores is well-constrained, vertical-axis rotations may be deduced from well-dated paleolatitude-only data of drill locations spread throughout the plate.

7. Conclusions

We reported new paleomagnetic data from Eocene, Oligocene and Miocene rocks from the island of Guam, located in the forearc region of the Izu-Bonin-Mariana subduction zone. These data include two Eocene poles that demonstrate rotation differences on Guam of as much as 35°, revealing that local rotations related to forearc deformation likely occurred. We include our new data into a compilation of previously published paleomagnetic data from the Philippine Sea Plate. Based on our paleomagnetic results and a critical re-evaluation of existing data we conclude that:

1) It cannot be established to which extent paleomagnetic declinations from the Philippine Mobile Belt, the northern Maluku Islands, and the Izu-Bonin-Marianas forearc provide evidence of plate-wide rotation. Regional rotations demonstrably play a role, and

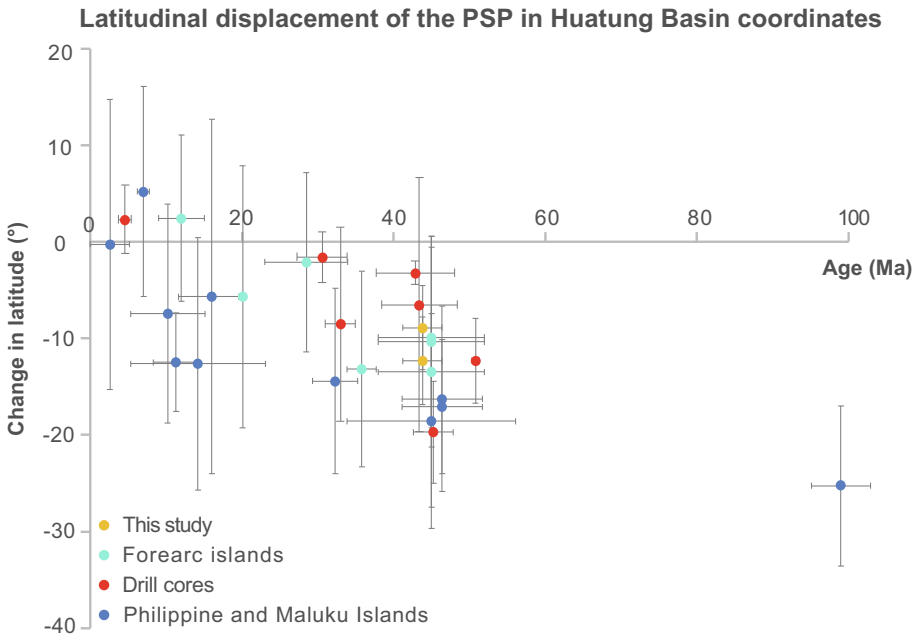

Fig. 8. Graph showing the change in latitude versus age, showing a more southerly position (negative latitudes) of the PSP back in time. The data is plotted in a 'Huatung Basin reference frame' to correct for intra-PSP plate motions (see Discussion section). Paleolatitudes are colored by general sampling location.

unequivocally robust data from the plate interior are currently not available.

2) The inclination-only data from igneous rocks are satisfied by a reconstruction in which all microplates of the Philippine Sea Plate are reconstructed relative to the Huatung Basin, and the for the latter a c. 15° northward motion since the mid-Eocene is reconstructed.
3) Drill-core paleomagnetic data with large sample sets from the stable plate interior are promising for future efforts to constrain the motion history of the Philippine Sea Plate. However, inclination shallowing should be corrected for, and uncertainties with for instance using the present-day field to correct for drill core rotation should be propagated into the analysis.
4) The paleomagnetic database does not require vertical axis rotations but does not preclude them.
5) Kinematic reconstructions of the Philippine Sea Plate should, for now, develop from systematic restorations of the geological records accreted at plate boundaries.

CRediT authorship contribution statement

Suzanna H.A. van de Lagemaat: Writing – review & editing, Writing – original draft, Visualization, Project administration, Investigation, Formal analysis, Data curation, Conceptualization. **Daniel Pastor-Galán:** Writing – review & editing, Validation, Formal analysis. **Bas B.G. Zanderink:** Investigation. **Maria J.Z. Villareal:** Writing – review & editing, Investigation. **John W. Jenson:** Supervision, Resources, Investigation. **Mark J. Dekkers:** Writing – review & editing, Writing – original draft, Formal analysis. **Douwe J.J. van Hinsbergen:** Writing – review & editing, Writing – original draft, Supervision, Funding acquisition, Formal analysis, Conceptualization.

Declaration of Competing Interest

The authors declare that they have no known competing financial interests or personal relationships that could have appeared to influence the work reported in this paper.

Data availability

Data are available in the supplementary information and via the Paleomagnetism.org and MagIC databases

Acknowledgements

SHAvdL and DJJvH were funded by NWO Vici grant 865.17.001 to DJJvH. DPG is funded by a 'Ramón y Cajal' Fellowship (RYC2019-028244-I) and the grant KiTSuNE (PID2021-128801NA-I00) both funded by 'MCIN/AEI/ESF Investing in your future'. We thank Fagan Matthys and CJ Paulino for their help in the field.

Appendix A. Supplementary data

Supplementary data to this article can be found online at https://doi.org/10.1016/j.tecto.2023.230010.

References

Ali, J.R., Hall, R., 1995. Evolution of the boundary between the Philippine Sea Plate and Australia: palaeomagnetic evidence from eastern Indonesia. Tectonophysics 251 (1–4), 251–275.
Aurelio, M.A., Barrier, E., Rangin, C., Müller, C., 1991. The Philippine fault in the late Cenozoic tectonic evolution of the Bondoc-Masbate-N. Leyte area, Central Philippines. J. SE Asian Earth Sci. 6 (3–4), 221–238.
Balmater, H.G., Manalo, P.C., Faustino-Eslava, D.V., Queaño, K.L., Dimalanta, C.B., Guotana, J.M.R., Ramos, N.T., Payot, B.D., Yumul Jr., G.P., 2015. Paleomagnetism of the Samar Ophiolite: Implications for the cretaceous sub-equatorial position of the Philippine island arc. Tectonophysics 664, 214–224.
Bird, P., 2003. An updated digital model of plate boundaries. Geochem. Geophys. Geosyst. 4 (3).
Bleil, U., 1982. Paleomagnetism of deep sea drilling project Leg 60 sediments and igneous rocks from the Mariana Region. Deep Sea Drill. Proj. 60, 855–873.
Boschman, L.M., Van Hinsbergen, D.J., Langereis, C.G., Flores, K.E., Kamp, P.J., Kimbrough, D.L., Spakman, W., 2021. Reconstructing lost plates of the Panthalassa Ocean through paleomagnetic data from circum-Pacific accretionary orogens. Am. J. Sci. 321 (6), 907–954.
Dankers, P.H.M., Zijderveld, J.D.A., 1981. Alternating field demagnetization of rocks, and the problem of gyromagnetic remanence. Earth Planet. Sci. Lett. 53 (1), 89–92.
Deenen, M.H., Langereis, C.G., van Hinsbergen, D.J., Biggin, A.J., 2011. Geomagnetic secular variation and the statistics of palaeomagnetic directions. Geophys. J. Int. 186 (2), 509–520.

Deschamps, A., Lallemand, S., 2002. The West Philippine Basin: an eocene to early oligocene back arc basin opened between two opposed subduction zones. J. Geophys. Res. Solid Earth 107 (B12), EPM–1.
Dimalanta, C.B., Faustino-Eslava, D.V., Gabo-Ratio, J.A.S., Marquez, E.J., Padrones, J.T., Payot, B.D., Yumul Jr., G.P., 2020. Characterization of the proto-Philippine Sea Plate: evidence from the emplaced oceanic lithospheric fragments along eastern Philippines. Geosci. Front. 11 (1), 3–21.
Fisher, R.A., 1953. Dispersion on a sphere. Proceed. Royal Soc. London. Series A. Math. Phys. Sci. 217 (1130), 295–305.
Fuller, M., Haston, R., Almasco, J., 1989. Paleomagnetism of the Zambales ophiolite, Luzon, northern Philippines. Tectonophysics 168 (1–3), 171–203.
Fuller, M., Haston, R., Lin, J.L., Richter, B., Schmidtke, E., Almasco, J., 1991. Tertiary paleomagnetism of regions around the South China Sea. J. Southeast Asian Earth Sci. 6 (3–4), 161–184.
Gaina, C., Müller, D., 2007. Cenozoic tectonic and depth/age evolution of the Indonesian gateway and associated back-arc basins. Earth Sci. Rev. 83 (3–4), 177–203.
Gerritsen, D., Vaes, B., van Hinsbergen, D.J., 2022. Influence of data filters on the position and precision of paleomagnetic poles: what is the optimal sampling strategy? Geochem. Geophys. Geosyst. 23 (4) e2021GC010269.
Grommé, C.S., Wright, T.L., Peck, D.L., 1969. Magnetic properties and oxidation of iron-titanium oxide minerals in Alae and Makaopuhi lava lakes, Hawaii. J. Geophys. Res. 74 (22), 5277–5293.
Hall, R., 2002. Cenozoic geological and plate tectonic evolution of SE Asia and the SW Pacific: computer-based reconstructions, model and animations. J. Asian Earth Sci. 20 (4), 353–431.
Hall, R., Ali, J.R., Anderson, C.D., Baker, S.J., 1995a. Origin and motion history of the Philippine Sea Plate. Tectonophysics 251 (1–4), 229–250.
Hall, R., Ali, J.R., Anderson, C.D., 1995b. Cenozoic motion of the Philippine Sea Plate: Palaeomagnetic evidence from eastern Indonesia. Tectonics 14 (5), 1117–1132.
Haston, R.B., Fuller, M., 1991. Paleomagnetic data from the Philippine Sea plate and their tectonic significance. J. Geophys. Res. Solid Earth 96 (B4), 6073–6098.
Haston, R., Fuller, M., Schmidtke, E., 1988. Paleomagnetic results from Palau, West Caroline Islands: a constraint on Philippine Sea plate motion. Geology 16 (7), 654–657.
Haston, R.B., Stokking, L.B., Ali, J., 1992. 31. Paleomagnetic data from holes 782A, 784A, and 786A, Leg 125. Proc. Ocean Drill. Program Sci. Results 125, 535–545.
Hickey-Vargas, R., 1998. Origin of the Indian Ocean-type isotopic signature in basalts from Philippine Sea plate spreading centers: an assessment of local versus large-scale processes. J. Geophys. Res. Solid Earth 103 (B9), 20963–20979.
Hickey-Vargas, R., 2005. Basalt and tonalite from the Amami Plateau, northern West Philippine Basin: New early cretaceous ages and geochemical results, and their petrologic and tectonic implications. Island Arc 14 (4), 653–665.
Hickey-Vargas, R., Ishizuka, O., Bizimis, M., 2013. Age and geochemistry of volcanic clasts from DSDP Site 445, Daito Ridge and relationship to Minami-Daito Basin and early Izu-Bonin arc magmatism. J. Asian Earth Sci. 70, 193–208.
Hickey-Vargas, R., Yogodzinski, G.M., Ishizuka, O., McCarthy, A., Bizimis, M., Kusano, Y., Arculus, R., 2018. Origin of depleted basalts during subduction initiation and early development of the Izu-Bonin-Mariana island arc: evidence from IODP expedition 351 site U1438, Amami-Sankaku basin. Geochim. Cosmochim. Acta 229, 85–111.
Hilde, T.W., Chao-Shing, L., 1984. Origin and evolution of the West Philippine Basin: a new interpretation. Tectonophysics 102 (1–4), 85–104.
Ishizuka, O., Yuasa, M., Tamura, Y., Shukuno, H., Stern, R.J., Naka, J., Taylor, R.N., 2010. Migrating shoshonitic magmatism tracks Izu–Bonin–Mariana intra-oceanic arc rift propagation. Earth Planet. Sci. Lett. 294 (1–2), 111–122.
Ishizuka, O., Tani, K., Reagan, M.K., Kanayama, K., Umino, S., Harigane, Y., Dunkley, D. J., 2011a. The timescales of subduction initiation and subsequent evolution of an oceanic island arc. Earth Planet. Sci. Lett. 306 (3–4), 229–240.
Ishizuka, O., Taylor, R.N., Yuasa, M., Ohara, Y., 2011b. Making and breaking an island arc: a new perspective from the Oligocene Kyushu-Palau arc, Philippine Sea. Geochem. Geophys. Geosyst. 12 (5).
Ishizuka, O., Taylor, R.N., Ohara, Y., Yuasa, M., 2013. Upwelling, rifting, and age-progressive magmatism from the Oki-Daito mantle plume. Geology 41 (9), 1011–1014.
Ishizuka, O., Hickey-Vargas, R., Arculus, R.J., Yogodzinski, G.M., Savov, I.P., Kusano, Y., Sudo, M., 2018. Age of Izu–Bonin–Mariana arc basement. Earth Planet. Sci. Lett. 481, 80–90.
Ishizuka, O., Tani, K., Taylor, R.N., Umino, S., Sakamoto, I., Yokoyama, Y., Sekimoto, S., 2022. Origin and age of magmatism in the northern Philippine Sea basins. Geochem. Geophys. Geosyst. 23 (4).
Jarboe, N.A., Koppers, A.A., Tauxe, L., Minnett, R., Constable, C., 2012. The online MagIC Database: data archiving, compilation, and visualization for the geomagnetic, paleomagnetic and rock magnetic communities, (GP31A-1063).. AGU Fall Meeting Abstracts.
Johnson, C.L., Constable, C.G., Tauxe, L., Barendregt, R., Brown, L.L., Coe, R.S., Stone, D. B., 2008. Recent investigations of the 0–5 Ma geomagnetic field recorded by lava flows. Geochem. Geophys. Geosyst. 9 (4).
Keating, B., 1980. Paleomagnetic study of sediments from deep sea drilling project leg 59. In: Kroenke, L., Scott, R., et al. (Eds.), Init. Repts. DSDP, 59, pp. 523–532.
Keating, B.H., Helsley, C.E., 1985. Implications of island arc rotations to the studies of marginal terranes. J. Geodyn. 2 (2–3), 159–181.
Keating, B.H., Herrero, E., 1980. Palcomagnetic studies of basalts and andesites from DSDP Leg 59. Initial Rep. Deep Sea Drill. Proj. 59, 533–544.
Keating, B., Kodama, K, Uyeda, S., Helsley, C.E., 1983. Paleomagnetic studies of the Bonin and Mariana island arcs. Arc Volcanism: Physics and Tectonics, Advances in Earth and Planetary Sciences Series 243–259.
Kinoshita, H., 1980. Paleomagnetism of sediment cores from Deep Sea Drilling Project Leg 58, Philippine Sea. In: *Init. Rept.,* DSDP, 58, pp. 765–768.
Kirschvink, J., 1980. The least-squares line and plane and the analysis of palaeomagnetic data. Geophys. J. Int. 62 (3), 699–718.
Kodama, K., Keating, B.H., Helsley, C.E., 1983. Paleomagnetism of the Bonin Islands and its tectonic significance. Tectonophysics 95 (1–2), 25–42.
Koyama, M., Cisowski, S.M., Pezard, P.A. (Eds.), 1992. Paleomagnetic evidence for northward drift and clockwise rotation of the Izu-Bonin Forearc since the early Oligocene, in Proceedings of the Ocean Drilling Program, Bonin Arc-Trench System; Covering Leg 126 of the Cruises of the Drilling Vessel JOIDES Resolution, Tokyo, Japan to Tokyo, Japan, Sites 787–793, 18 April 1989–19 June 1989. Tex. A & M Univ., Ocean Drill, Program, College Station, Tex, pp. 353–370.
Koymans, M.R., Langereis, C.G., Pastor-Galán, D., van Hinsbergen, D.J., 2016. Paleomagnetism. Org: an online multi-platform open source environment for paleomagnetic data analysis. Comput. Geosci. 93, 127–137.
Koymans, M.R., van Hinsbergen, D.J.J., Pastor-Galán, D., Vaes, B., Langereis, C.G., 2020. Towards FAIR paleomagnetic data management through Paleomagnetism. Org 2.0. Geochem. Geophys. Geosyst. 21 (2) e2019GC008838.
Liu, W., Gai, C., Feng, W., Cao, W., Guo, L., Zhong, Y., Liu, Q., 2021. Coeval evolution of the eastern Philippine Sea Plate and the South China Sea in the early Miocene: paleomagnetic and provenance constraints from ODP site 1177. Geophys. Res. Lett. 48 (14) e2021GL093916.
Liu, J., Li, S., Cao, X., Dong, H., Suo, Y., Jiang, Z., Foulger, G.R., 2023. Back-arc tectonics and plate reconstruction of the Philippine Sea-South China Sea region since the eocene. Geophys. Res. Lett. 50 (5) e2022GL102154.
Louden, K.E., 1977. Paleomagnetism of DSDP sediments, phase shifting of magnetic anomalies, and rotations of the West Philippine Basin. J. Geophys. Res. 82 (20), 2989–3002.
McCabe, R., Uyeda, S., 1983. Hypothetical model for the bending of the Mariana Arc. In: Washington DC American Geophysical Union Geophysical Monograph Series, 27, pp. 281–293.
McFadden, P.L., McElhinny, M.W., 1988. The combined analysis of remagnetization circles and direct observations in palaeomagnetism. Earth Planet. Sci. Lett. 87 (1–2), 161–172.
Meert, J.G., Pivarunas, A.F., Evans, D.A., Pisarevsky, S.A., Pesonen, L.J., Li, Z.X., Salminen, J.M., 2020. The magnificent seven: a proposal for modest revision of the quality index. Tectonophysics 790, 228549.
Meijer, A., Reagan, M., Ellis, H., Shafiqullah, M., Sutter, J., Damon, P., Kling, S., 1983. Chronology of volcanic events in the eastern Philippine Sea. In: Washington DC American Geophysical Union Geophysical Monograph Series, 27, pp. 349–359.
Morishita, T., Tani, K.I., Soda, Y., Tamura, A., Mizukami, T., Ghosh, B., 2018. The uppermost mantle section below a remnant proto-Philippine Sea island arc: insights from the peridotite fragments from the Daito Ridge. Am. Mineral. J. Earth Planet. Mater. 103 (7), 1151–1160.
Mullender, T.A.T., Van Velzen, A.J., Dekkers, M.J., 1993. Continuous drift correction and separate identification of ferrimagnetic and paramagnetic contributions in thermomagnetic runs. Geophys. J. Int. 114 (3), 663–672.
Mullender, T.A., Frederichs, T., Hilgenfeldt, C., de Groot, L.V., Fabian, K., Dekkers, M.J., 2016. Automated paleomagnetic and rock magnetic data acquisition with an in-line horizontal "2 G" system. Geochem. Geophys. Geosyst. 17 (9), 3546–3559.
NOAA National Centers for Environmental Information, 2022. ETOPO 2022 15 Arc-Second Global Relief Model. NOAA National Centers for Environmental Information.
Pubellier, M., Bader, A.G., Rangin, C., Deffontaines, B., Quebral, R., 1999. Upper plate deformation induced by subduction of a volcanic arc: the Snellius Plateau (Molucca Sea, Indonesia and Mindanao, Philippines). Tectonophysics 304 (4), 345–368.
Queaño, K.L., Ali, J.R., Milsom, J., Aitchison, J.C., Pubellier, M., 2007. North Luzon and the Philippine Sea Plate motion model: Insights following paleomagnetic, structural, and age-dating investigations. J. Geophys. Res. Solid Earth 112 (B5).
Queaño, K.L., Ali, J.R., Pubellier, M., Yumul Jr., G.P., Dimalanta, C.B., 2009. Reconstructing the mesozoic-early cenozoic evolution of northern Philippines: clues from palaeomagnetic studies on the ophiolitic basement of the Central Cordillera. Geophys. J. Int. 178 (3), 1317–1326.
Reagan, M.K., Meijer, A., 1984. Geology and geochemistry of early arc-volcanic rocks from Guam. Geol. Soc. Am. Bull. 95 (6), 701–713.
Reagan, M.K., Ishizuka, O., Stern, R.J., Kelley, K.A., Ohara, Y., Blichert-Toft, J., Woods, M., 2010. Fore-arc basalts and subduction initiation in the Izu-Bonin-Mariana system. Geochem. Geophys. Geosyst. 11 (3).
Reagan, M.K., McClelland, W.C., Girard, G., Goff, K.R., Peate, D.W., Ohara, Y., Stern, R. J., 2013. The geology of the southern Mariana fore-arc crust: implications for the scale of Eocene volcanism in the western Pacific. Earth Planet. Sci. Lett. 380, 41–51.
Reagan, M.K., Heaton, D.E., Schmitz, M.D., Pearce, J.A., Shervais, J.W., Koppers, A.A., 2019. Forearc ages reveal extensive short-lived and rapid seafloor spreading following subduction initiation. Earth Planet. Sci. Lett. 506, 520–529.
Richter, C., Ali, J.R., 2015. Philippine sea plate motion history: eocene-recent record from ODP Site 1201, central West Philippine basin. Earth Planet. Sci. Lett. 410, 165–173.
Sager, W.W., Carvallo, C., 2022. Paleomagnetism and paleolatitude of igneous drill core samples from the Izu-Bonin forearc and implications for Philippine Sea plate motion. Tectonophysics 841, 229573.
Sdrolias, M., Roest, W.R., Müller, R.D., 2004. An expression of Philippine Sea plate rotation: the Parece Vela and Shikoku basins. Tectonophysics 394 (1–2), 69–86.
Seno, T., Maruyama, S., 1984. Paleogeographic reconstruction and origin of the Philippine Sea. Tectonophysics 102 (1–4), 53–84.
Seton, M., Müller, R.D., Zahirovic, S., Gaina, C., Torsvik, T., Shephard, G., Talsma, A., Gurnis, M., Turner, M., Maus, S., Chandler, M., 2012. Global continental and ocean basin reconstructions since 200 Ma. Earth Sci. Rev. 113 (3–4), 212–270.

Siegrist, H.G., Reagan, M.K., RH, R., JW, J., 2008. Geologic map and sections of Guam. In: Mariana Islands (1: 50,000), Revision of original map from USGS Professional Report A, 403, p. 1964.
Tauxe, L., 2010. Essentials of Paleomagnetism. Univ of California Press.
Tauxe, L., Kent, D.V., 2004. A simplified statistical model for the geomagnetic field and the detection of shallow bias in paleomagnetic inclinations: was the ancient magnetic field dipolar? Geophys. Monogr. Series 145, 101–115.
Tracey Jr., J.I., Schlanger, S.O., Stark, J.T., Doan, D.B., May, H.G., 1964. *General Geology of Guam* (No. 403-A).
Vaes, B., Li, S., Langereis, C.G., van Hinsbergen, D.J., 2021. Reliability of palaeomagnetic poles from sedimentary rocks. Geophys. J. Int. 225 (2), 1281–1303.
Vaes, B., Gallo, L.C., van Hinsbergen, D.J., 2022. On pole position: causes of dispersion of the paleomagnetic poles behind apparent polar wander paths. J. Geophys. Res. Solid Earth 127 (4) e2022JB023953.
Van Hinsbergen, D.J.J., Dekkers, M.J., Bozkurt, E., Koopman, M., 2010. Exhumation with a twist: Paleomagnetic constraints on the evolution of the Menderes metamorphic core complex, western Turkey. Tectonics 29 (3).
Wu, J., Suppe, J., Lu, R., Kanda, R., 2016. Philippine Sea and East Asian plate tectonics since 52 Ma constrained by new subducted slab reconstruction methods. J. Geophys. Res. Solid Earth 121 (6), 4670–4741.
Wu, J., Lin, Y.A., Flament, N., Wu, J.T.J., Liu, Y., 2022. Northwest Pacific-Izanagi plate tectonics since cretaceous times from western Pacific mantle structure. Earth Planet. Sci. Lett. 583, 117445.
Xu, J., Ben-Avraham, Z., Kelty, T., Yu, H.S., 2014. Origin of marginal basins of the NW Pacific and their plate tectonic reconstructions. Earth Sci. Rev. 130, 154–196.
Yamazaki, T., Seama, N., Okino, K., Kitada, K., Joshima, M., Oda, H., Naka, J., 2003. Spreading process of the northern Mariana Trough: rifting-spreading transition at 22 N. Geochem. Geophys. Geosyst. 4 (9).
Yamazaki, T., Takahashi, M., Iryu, Y., Sato, T., Oda, M., Takayanagi, H., Chiyonobu, S., Nishimura, A., Nakazawa, T., Ooka, T., 2010. Philippine Sea Plate motion since the Eocene estimated from paleomagnetism of seafloor drill cores and gravity cores. Earth, Planets and Space 62 (6), 495–502.
Yamazaki, T., Chiyonobu, S., Ishizuka, O., Tajima, F., Uto, N., Takagawa, S., 2021. Rotation of the Philippine Sea plate inferred from paleomagnetism of oriented cores taken with an ROV-based coring apparatus. Earth, Planets and Space 73 (1), 1–10.
Yumul Jr., G.P., Dimalanta, C.B., Gabo-Ratio, J.A.S., Queaño, K.L., Armada, L.T., Padrones, J.T., Marquez, E.J., 2020. Mesozoic rock suites along western Philippines: exposed proto-South China Sea fragments? J. Asian Earth Sci. X 4, 100031.
Zahirovic, S., Seton, M., Müller, R.D., 2014. The cretaceous and cenozoic tectonic evolution of Southeast Asia. Solid Earth 5 (1), 227–273.
Zijderveld, J.D.A., 1967. The natural remanent magnetizations of the Exeter volcanic traps (Permian, Europe). Tectonophysics 4 (2), 121–153.